JTTEE5 16:488–497
DOI: 10.1007/s11666-007-9060-5
1059-9630/$19.00 © ASM International

Microstructural Studies of Cold Sprayed Copper, Nickel, and Nickel-30% Copper Coatings

Heli Koivuluoto, Juha Lagerbom, and Petri Vuoristo

(Submitted November 2, 2006; in revised form April 23, 2007)

Cold spraying enables to produce metallic coatings with low porosity level and low oxygen content. Several material properties such as electrical conductivity and corrosion resistance rely on these properties. Aim of this study was to characterize microstructural properties of cold sprayed copper, nickel, and nickel-30%copper coatings. Microstructures, denseness, and deformation of particles were investigated. SEM analysis and corrosion tests were done to get information of through-porosity. Open porosity has an important role on protectiveness of anodically protective coatings, such coating materials like copper and nickel. In this study, cold-sprayed Cu coating was fully dense. However, cold-sprayed Ni and Ni-30%Cu coatings seemed to be microstructurally dense but some porosity in some areas of the coatings especially in some parts of particle boundaries was noticed after corrosion tests. Furthermore, effect of annealing to microstructure and corrosion test behavior was studied. Cold sprayed Ni coating became denser during heat treatment.

Keywords cold gas dynamic spraying, corrosion test, copper nickel, microstructure, nickel-30% copper

1. Introduction

In the cold spray process, a gas is accelerated to supersonic velocity by a converging-diverging de Laval type nozzle (Ref 1). Formation of a cold-sprayed coating depends on the velocity of powder particles. Each material has a specific critical velocity v_{cr}. Above v_{cr} the particles adhere to the substrate causing plastic deformation and formation of the coating. At velocities lower than v_{cr} only erosion and particle rebounding occur with no coating building up (Ref 1, 2). In cold spraying, several parameters such as the particle size (typically 5-25 μm), particle temperature, substrate material, and the properties of the coating material have a remarkable influence on the formation and the deposition efficiency (Ref 1, 3, 4). Good bonding between the cold sprayed powder particles needs heavy plastic deformation during the particle impact (Ref 2, 4). Upon impact the solid particles deform and bond together, forming a coating (Ref 2). For successful bonding, deposition conditions in which oxide layers on the particle surfaces are destroyed during impact should be created (Ref 4). The powder particles impinge on the substrate in solid form, well below the powder melting temperature (Ref 2). Wide range of coating and substrate materials, e.g., pure metals, metal alloys, polymers, and composites, can be used in cold spraying (Ref 3). As a materials processing method, cold spraying is kept very similar to an explosive welding (Ref 5).

Cold spraying enables production of metallic coatings with very low porosity level and low oxygen content. Cold spraying is also an effective method to deposit dense and pure coatings (Ref 6). This is regarded as an advantage for several important material properties such as electrical conductivity and corrosion resistance (Ref 1). According to Stoltenhoff et al. (Ref 1) electrical conductivity of the cold sprayed copper is about 90% of the value of pure copper. Published studies on corrosion resistance of cold sprayed coatings are so far very rare, and have been reported only for Zn, Al, or Zn-Al composite coatings. Recently Blose et al. (Ref 7) reported that such coatings can protect steel substrates from wet corrosion. Sacrificial corrosion of Al in the cold sprayed Al coating and formation of thin $ZnCl_2$ layer through cathodic protection in the cold sprayed Zn coatings was found to protect steel in a chloride environment. Salt spray (fog) testing is a commonly used test method to evaluate the quality of various coatings. This particular test enables using different corrosive solutions and different test temperatures in a controlled test condition (Ref 8). In the present work, the studies are more focused on corrosion properties of anodically protective coatings instead of cathodically protective coatings.

It is known that cold sprayed coatings have hardnesses somewhat higher than in corresponding bulk materials, due to high degree of work hardening. The coatings possess also high adherence to base materials and low thermal stresses due to low particle temperatures (Ref 2). According to

Heli Koivuluoto, Juha Lagerbom, and **Petri Vuoristo,** Laboratory of Surface Engineering, Institute of Materials Science, Tampere University of Technology, PO Box 589, 33101 Tampere, Finland. Contact e-mail: heli.koivuluoto@tut.fi.

Calla et al. (Ref 5), the reason to high hardness of the cold sprayed coatings is the very fine grain size and the significant microstrain in the as-sprayed deposits. Annealing at elevated temperatures affects the properties of cold sprayed coatings. At temperatures of 300 °C and above for Cu, the dislocations in the grains rearrange, and recrystallization and further grain growth occur. A decrease in the hardness is usually the result (Ref 5).

In the present study characteristics of the cold sprayed copper, nickel, and nickel-30%copper (Monel 400) coatings were investigated. Aim of this study was to investigate the microstructure and degree of impermeability of coatings prepared by cold spraying. Denseness of the cold sprayed coatings was evaluated by wet corrosion testing, which is able to detect the existing through-porosity (open-porosity) in the coatings. The corrosion tests used were open cell potential measurements and salt spray fog testing. The structural integrity is important for several coating properties. Cold sprayed copper was chosen because of its interesting conductivity properties for electrical and heat conductivity applications. Nickel and nickel-30%copper coatings were chosen because of their potential in applications requiring good corrosion resistances. The substrate material used in the study was carbon steel. The effect of heat treatment to the different properties was also studied.

2. Experimental Procedure

2.1 Spraying Parameters

The cold sprayed coatings were prepared at Linde AG Linde Gas Division (Unterschleissheim, Germany). The cold spray system used was Kinetiks 3000 M with a standard gun nozzle (Cold Gas Technology GmbH, CGT, Germany). Nitrogen, helium, or mixture of them can be used as the process gas in the equipment. The gas pressure can be controlled in the range of 15-40 bar and the gas pre-heating temperature at 200-800 °C. The summary of the cold spraying parameters used in the present work is presented in Table 1. In this study, nitrogen was used as the process gas. Reference samples were HVOF sprayed with a Sulzer Metco Diamond Jet Hydrid 2700 gun. The HVOF spray parameters were oxygen flow rate of 202 l/min for Cu and 215 l/min for Ni and Ni-30%Cu, propane flow rate of 74 l/min, air flow rate of 391 l/min, powder feed rate of 60 g/min, surface velocity of 183 m/min, spraying distance 230 mm, and 48 spray layers with a rotating sample holder. Coating thickness of HVOF Cu, Ni, and Ni-30%Cu sprayed coatings was 320, 570, 285 μm, respectively.

2.2 Powders

The powders used in this study were copper, nickel, and nickel-30%copper alloy (Monel 400), see Table 2. Three different copper powders were used. They were purchased from two different suppliers and had three different particle sizes. The Ni and Ni-30%Cu powders selected were typical powders with good sprayability in the cold spray process. All powders were manufactured by gas atomization. Powders used for the reference samples were Cu (Sulzer Metco, Metco Diamalloy 1007, −88 + 31 μm), Ni (Sulzer Metco 56F NS, −45 + 10 μm), and Ni-30%Cu (Sandvik Osprey, −38 + 16 μm).

The three Cu, Ni, and Ni-30%Cu powders were sprayed onto grit blasted (18 mesh) steel substrates. Figure 1 shows the morphology of the BSA Cu (−22 + 5 μm) powder. Morphologies of the BSA Cu (−38 + 11 μm) and the Osprey Cu (−30 + 10 μm) are presented in Figs. 2 and 3, respectively. The particle size distribution of the Osprey Cu powder was smaller than the distribution of the BSA powders. Moreover, powders produced by BSA include smaller particles more than the Osprey Cu powder. Ni particles were spherical in shape, with few agglomerates also present (Fig. 4). Ni-30%Cu powder contained a lot of agglomerates (satellites) and also significantly more very small particles as compared to the nominal particle size given by the powder producer. Thus, the particle size distribution was relatively large (Fig. 5).

2.3 Sample Preparation

Samples had to be etched in order to see the real microstructures of the cold sprayed coatings. Table 3 presents the etching conditions for each coating material. The Ni coating was etched in a boiling solution.

2.4 Characterization of the Cold Sprayed Coatings

Microstructures of the cold sprayed coatings were investigated with a Philips XL30 scanning electron microscope (SEM). Microstructures of the cold sprayed coatings were studied from unetched and etched cross-sectional coating samples. Corrosion behavior and especially the through-porosity (impermeability) of the cold sprayed coatings were tested with open cell potential measurements and salt spray (fog) testing. Two plastic tubes were glued on the surface of the coating sample for the open cell potential measurements. The diameter of tube was 20 mm. An amount of 12 ml of 3.5 wt%

Table 1 Cold spray parameters and coating thicknesses

Material	Pressure (bar)	Total N_2 flow rate (m^3/h)	Temperature (°C)	Coating thickness (μm)
Cu (BSA −22 + 5)	28	70	320	520
Cu (BSA −38 + 11)	28	73	420	430
Cu (Osprey −30 + 10)	28	80	400	440
Ni	28	61	500	320
Ni-30%Cu	28, 30	64, 70	450, 525	150, 510

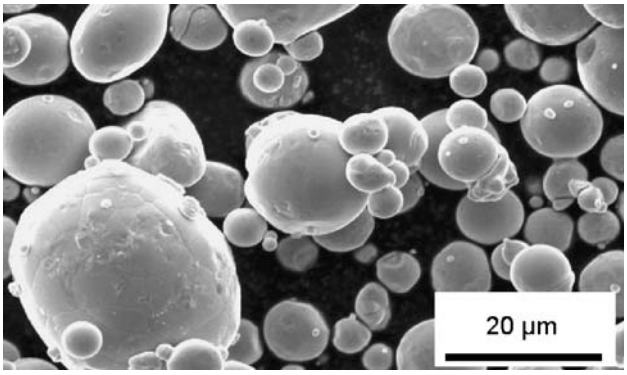

Fig. 1 Morphology of Cu powder (BSA −22 + 5 μm)

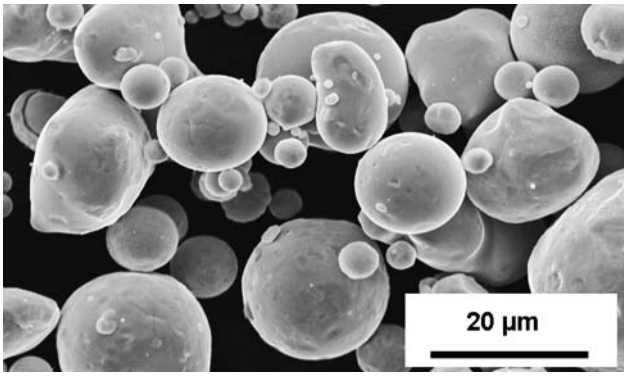

Fig. 2 Morphology of Cu powder (BSA −38 + 11 μm)

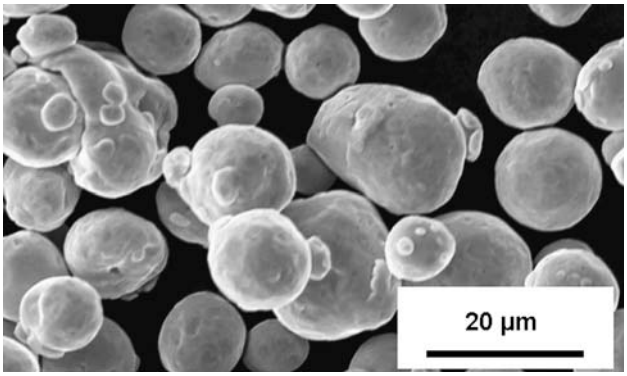

Fig. 3 Morphology of Cu powder (Osprey −30 + 10 μm)

Table 2 Spray powders used in cold spraying

Material	Particle size (μm)	Producer	Production Method
Cu	−22 + 5	BSA Metals	Gas atomized
Cu	−38 + 11	BSA Metals	Gas atomized
Cu	−30 + 10	Sandvik Osprey	Gas atomized
Ni	−25 + 5	H. C. Starck	Gas atomized
Ni-30%Cu	−38 + 16	Sandvik Osprey	Gas atomized

All particle sizes are nominal values given by the producer

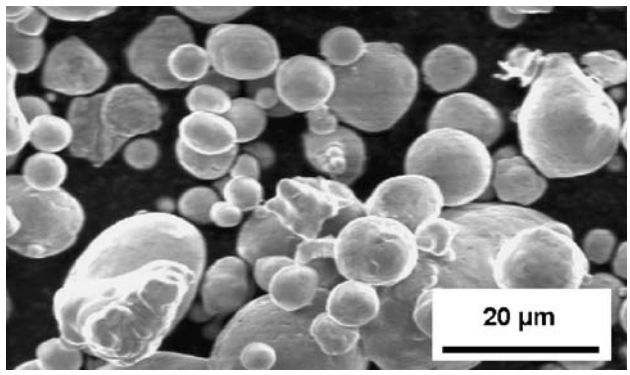

Fig. 4 Morphology of Ni powder

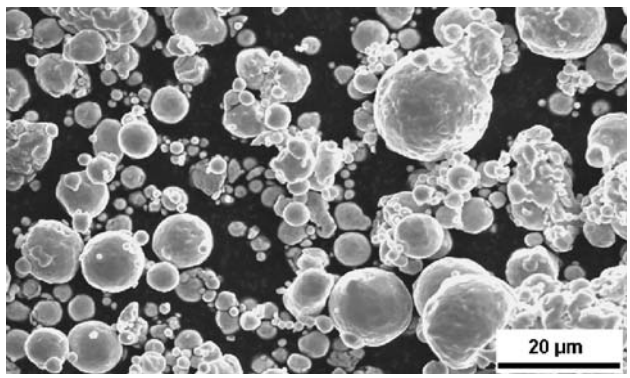

Fig. 5 Morphology of Ni-30%Cu powder

Table 3 Etching conditions for cold sprayed coatings

Material	Etching solution	Time (s)	Boiling solution
Cu	95 ml ethanol 5 g $FeCl_3$ 2 ml HCl	90	No
Ni	10 ml glycerol 5 ml HNO_3 15 ml HCl	3	Yes
Ni-30%Cu	99 ml ethanol 5 g $FeCl_3$ 2 ml HCl	40	No

NaCl-solution was filled into the tubes. Measurement period was 9 days. Open cell measurements were done with Fluke 79 III true RMS-multimeter. Silver/silver chloride electrode was used as a reference electrode. Salt spray (fog) testing was done by following the ASTM B117 standard. 5 wt% NaCl-solution was used and exposure time was 96 h. Temperature was 35-40 °C, pH of the salt solution was 6.3 and accumulation of solution was 0.04 ml/cm^2 h during exposure. The samples were examined visually before, during and after exposure. Also cross-sectional SEM studies after corrosion test were performed. The effect of heat treatments on properties of the cold sprayed coatings was studied. Heat treatments were done in a

Carbolite 3-zone controlled atmosphere furnace using argon as the protective gas. Holding time at the annealing temperature was 5 h.

3. Results

3.1 Microstructure of Cold Sprayed Coatings

Microstructures of the as-sprayed and the heat-treated cold sprayed coatings on steel substrates are presented in Figs. 6-11. Figure 6 presents the microstructure of cold sprayed Cu coating sprayed from the fine size BSA powder with the particle size of $-22+5$ μm. The unetched microstructure of the coating is shown in Fig. 6a. Cu coatings sprayed from the two other powders had similar

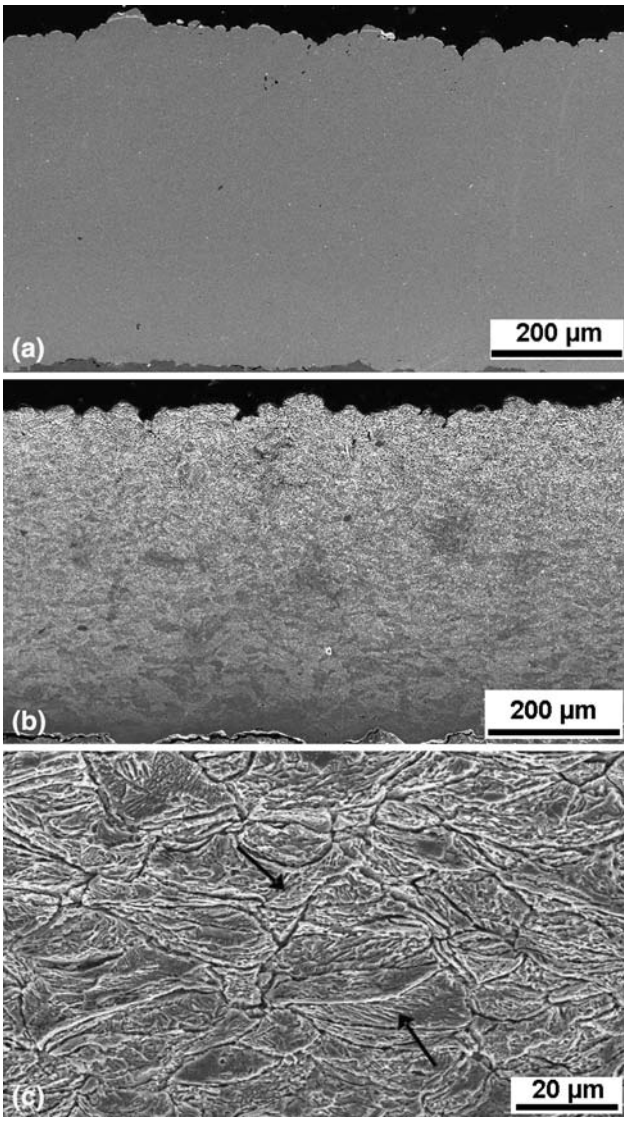

Fig. 6 Cold sprayed Cu coating (BSA $-22+5$ μm) on grit blasted steel (a) unetched, (b), and (c) etched. The arrows indicate the slip bands

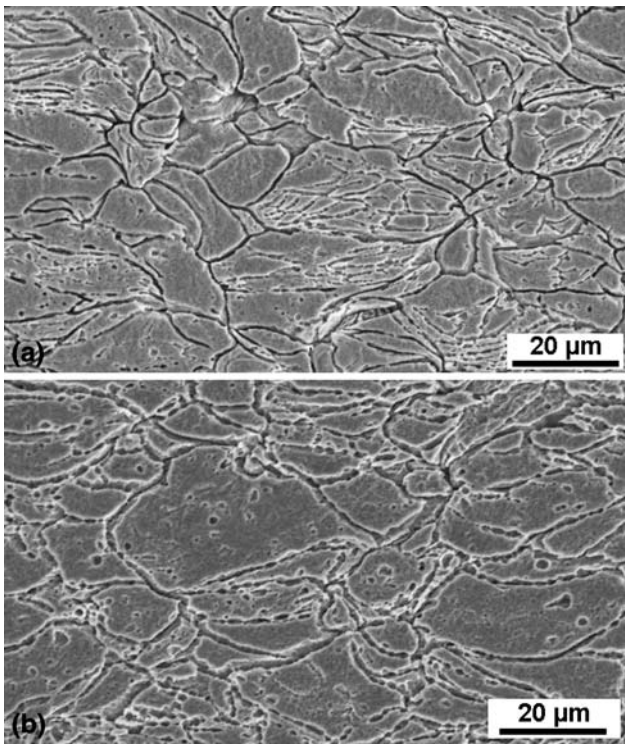

Fig. 7 Etched cold sprayed Cu coating (BSA $-22+5$ μm), at (a) 200 °C and (b) 400 °C heat-treated (5 h)

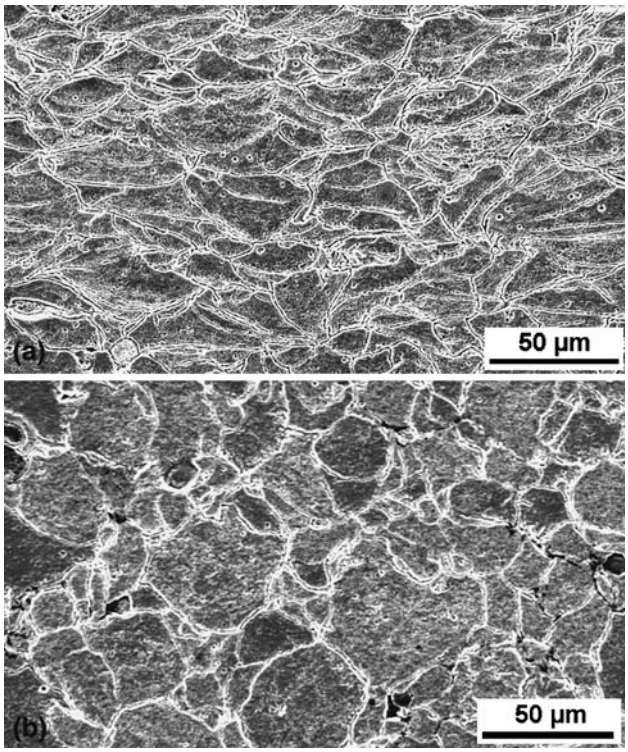

Fig. 8 Cold sprayed Cu coating (BSA $-38+11$ μm) (a) etched cross-sectional and (b) etched top-view microstructure

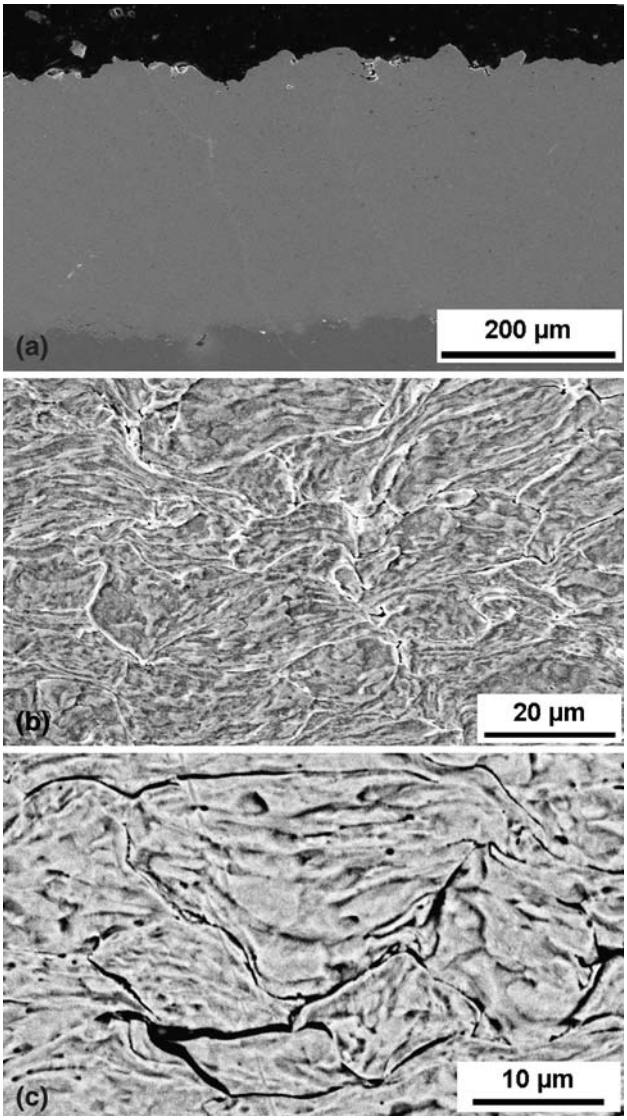

Fig. 9 Cold sprayed Ni coating on grit blasted steel (a) unetched, (b) etched, and (c) etched BSE image

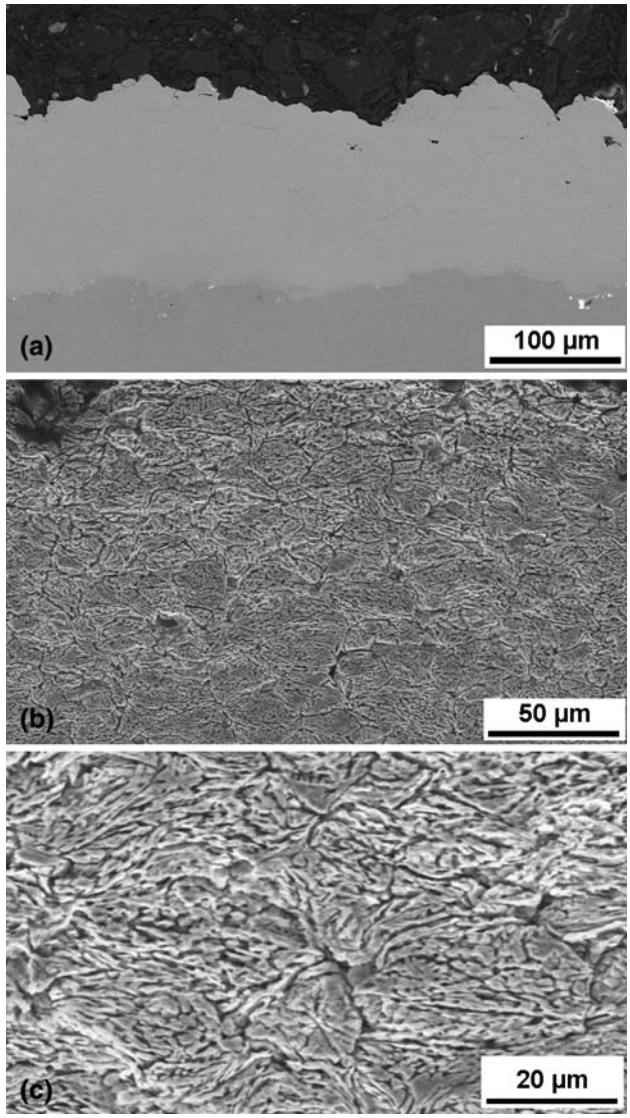

Fig. 10 Cold sprayed Ni-30%Cu coating on grit blasted steel (a) unetched, (b), and (c) etched

microstructures as that shown in Fig. 6a. All cold sprayed Cu coatings were found to be dense showing no signs of porosity or voids. Figures 6b and c present the etched microstructures of the cold sprayed Cu coating prepared from the fine size BSA powder. The particle boundaries and deformation present in the form of slip bands in the coating particles are seen in the etched microstructure. The actual grain size within the particles is not clearly seen. The sprayed particles show high degree of flattening when impacting the substrate or previously sprayed coating layer. Figure 7 presents the microstructure of a heat-treated cold sprayed Cu (BSA $-22+5$ μm) coating. The microstructures of cold sprayed Cu coatings heat-treated at 200 °C and 400 °C for 5 h are presented in Figs. 7a and b, respectively. At 200 °C some recrystallization has possibly taken place. This is seen as a noticeably lower amount of slip bands. The cold sprayed Cu coating heat-treated at 400 °C seems to have even less slip bands. Also the primary spray particles seem to be slightly larger. However, this needs to be verified with other characterization methods.

An etched microstructure of the cold sprayed Cu coating prepared from the slightly coarser BSA powder (BSA $-38+10$ μm) is presented in Fig. 8. Sample preparation from two different directions, i.e., from cross-section and from top of the coating, was also conducted. Shapes of particle splats in the etched cross-section sample were compared to the polished and etched top-view sample. Cross-sectional microstructure is presented in Fig. 8a and the top-view microstructure in Fig. 8b. Obviously, the shapes of the flattened and deformed particles are only seen from the cross-sectional view and not directly from the top-view.

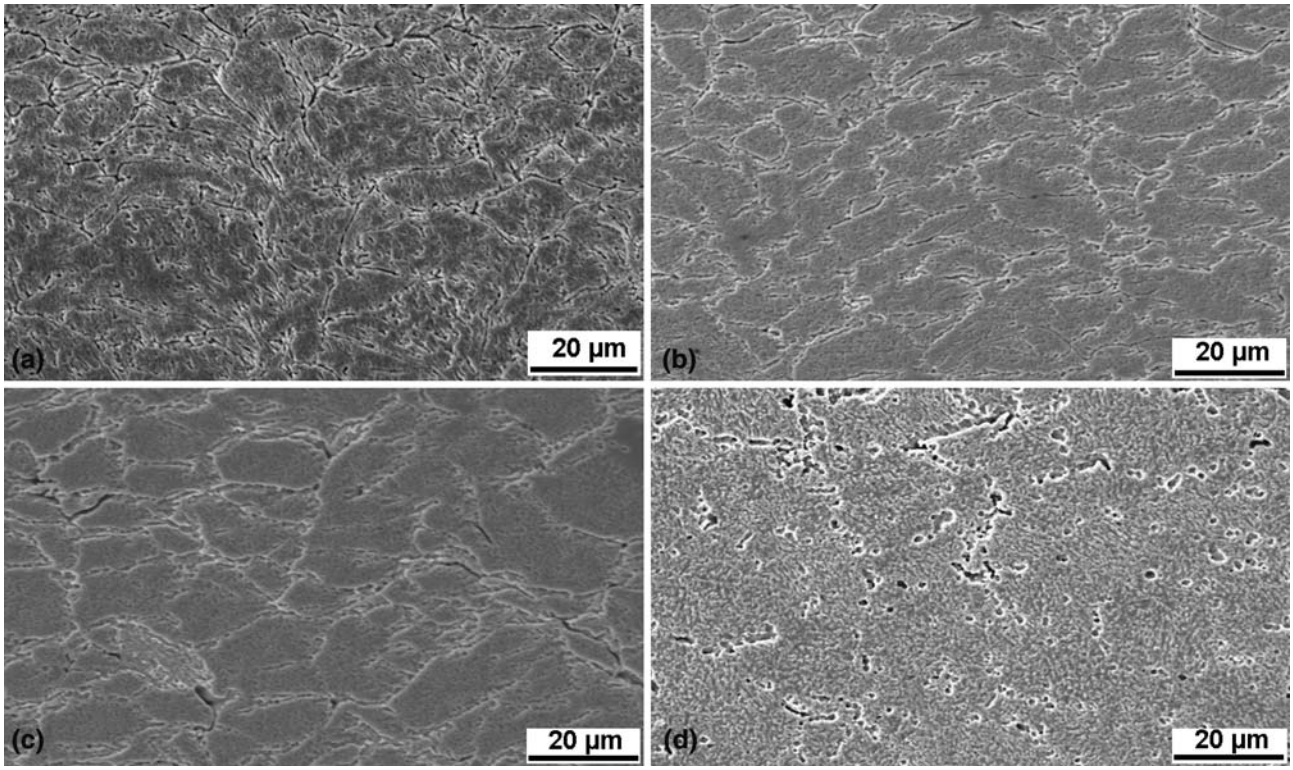

Fig. 11 Etched cold sprayed Ni-30%Cu coating, heat-treated (5 h) at (a) 400, (b) 600, (c) 800, and (d) 1000 °C

Microstructures of the cold sprayed Ni coating on grit blasted steel substrates are presented in Fig. 9. The cold sprayed Ni coating is microstructurally dense as studied by SEM. Very low amount of pores are seen in the coating microstructure, see Fig. 9a. An etched microstructure of the cold sprayed Ni coating is shown in Fig. 9b. Some particle boundaries and also grain boundaries due to the deformed material are also seen in the microstructure. The interface between the coating and the substrate was found to be mainly faultless and clean. Backscattering electron (BSE) image taken from an etched cold sprayed Ni coating is shown in Fig. 9c. The better contrast in the etched microstructure as compared to the secondary electron (SE) image (Fig. 9b) is apparently caused by the imaging method used.

The cold sprayed Ni-30%Cu coating on grit blasted steel substrate (unetched and etched microstructure) is presented in Fig. 10. This coating is also very dense with low amount of detectable pores and voids based on studies with SEM. The interface between the coating and the substrate is also mainly faultless. Some particle boundaries and also some microstructural details, possibly for example grain boundaries, are also seen in the etched specimen. Microstructures of the heat-treated cold sprayed Ni-30%Cu coatings are presented in Fig. 11. The heat treatment temperatures were 400, 600, 800, and 1000 °C. The duration of the heat treatment was 5 h. All coating specimen were etched under similar conditions, i.e., same time and etching solution. Particle boundaries were not so clearly seen with increasing heat treatment temperature. This may be a consequence of a denser cold sprayed coating with a low amount of inter-particle voids.

3.2 Denseness and Corrosion Characteristics of Cold Sprayed Coatings

More exact information about the denseness and especially about the through-porosity (open porosity) of the coatings was obtained by testing the corrosion behavior of the cold sprayed coatings. Cu, Ni and Ni-30%Cu coatings are known to give anodic protection to steel. Therefore, the open porosity has an important role on the protectiveness of such coatings on steel. The corrosion tests used in this work i.e., open cell potential measurements and salt spray (fog) testing, showed some through-porosity in the cold sprayed Ni and Ni-30%Cu coatings. These cold sprayed coatings had several areas in which the surfaces were uncorroded, which shows their potential as corrosion resistant coatings. However, both cold sprayed Ni and Ni-30%Cu coatings had several weak-points, which resulted local corrosion in the tests used in this work. Figure 12 presents the cross-sectional microstructure of the cold sprayed Ni-30%Cu coating after open cell potential measurements. The corrosion tests showed the local weak areas in the cold sprayed coatings. This coating area was chosen after corrosion test to indicate structural defects in the coating. A path for the electrolyte (3.5% NaCl solution) to penetrate into the coating and to the coating/substrate interface is partly seen in the centre of the SEM micrograph. With such imperfections the

corrosive salt solution is able to penetrate through the particle boundaries from the surface to the interface causing corrosion attack in the substrate material. Some areas at the interface between the coating and the substrate are clearly open possibly due to corrosion of substrate or imperfections on the interface. Corrosion products including iron oxides were found also on the surface of the coating.

The open cell potentials of the cold sprayed Cu coatings prepared from two coarse powders were similar to open cell potential of Cu bulk. The open cell potential of the cold sprayed Cu coating (BSA −22 + 5 μm) was closer to the potential of bulk Cu than that of the HVOF sprayed Cu coating. The open cell potential results were as follows: cold sprayed (CS) Cu coating −280 mV, HVOF sprayed Cu coating −500 mV, and wrought Cu −125 mV. Figure 13 presents the open cell potential behavior as a function of the exposure time for the Cu coatings and bulk material. The open cell potential of steel grade Fe52 was −700 mV. Open cell potential of different cold sprayed Cu coatings as compared to wrought Cu and Fe52 as a reference. Open cell potential of the coatings was quite close to the curve of Cu bulk material.

Through-porosity was found with the open cell potential measurements in the both Ni coatings. The open cell potential of the cold sprayed Ni coating was −520 mV and the HVOF sprayed Ni coating −400 mV. Electrolytically deposited standard Ni coating was chosen as a reference instead of bulk Ni and its potential was −260 mV. Open cell potential of heat-treated (400 °C and 5 h) cold sprayed Ni coating was close to the open cell potential of electrolytically deposited Ni coating (Fig. 14). The open cell potential of the as-sprayed cold sprayed Ni-30%Cu coating was −560 mV and the HVOF sprayed −260 mV, see Fig. 15. Open cell potential of the cold sprayed Ni-30%Cu coatings was near to same value after heat treatment (400 °C and 5 h) also.

Table 4 presents the summary of the visual examination of the cold sprayed and HVOF sprayed coatings on steel substrate after salt spray fog testing. Cold sprayed Cu coating was sprayed with the BSA (−22 + 5 μm) powder. The first changes detected on the coating surface during the test and the final state after exposure is shown in the table. According to the salt spray tests, the reference

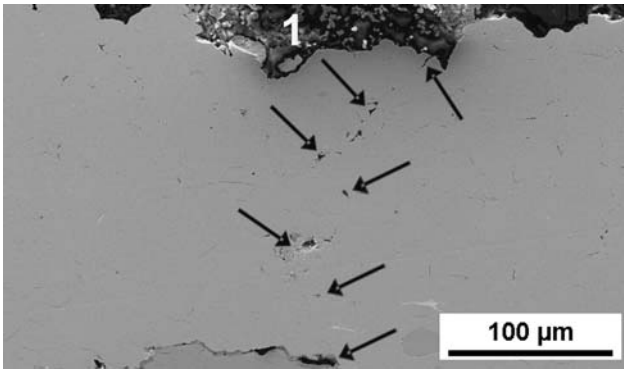

Fig. 12 Cold sprayed Ni-30%Cu coating after open cell potential measurements. Arrows indicate the possible penetrating bath. Interface seemed to be open and corrosion products (1) was seen on the top surface

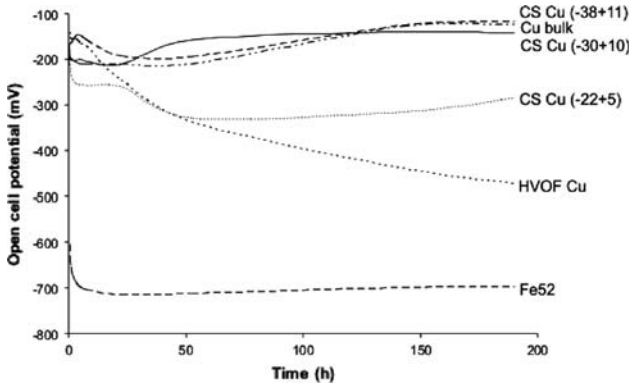

Fig. 13 Open cell potential of Cu bulk, reference Fe52, HVOF sprayed Cu, cold sprayed Cu (BSA −22 + 5 μm), cold sprayed Cu (BSA −38 + 11 μm), and cold sprayed Cu (Osprey −30 + 10 μm) as a function of exposure time

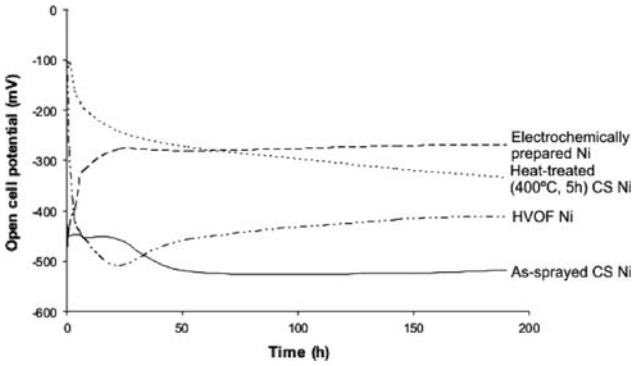

Fig. 14 Open cell potential of cold sprayed Ni coatings as-sprayed and heat-treated (400 °C and 5 h) and electrolytically prepared Ni coating as a function of exposure time

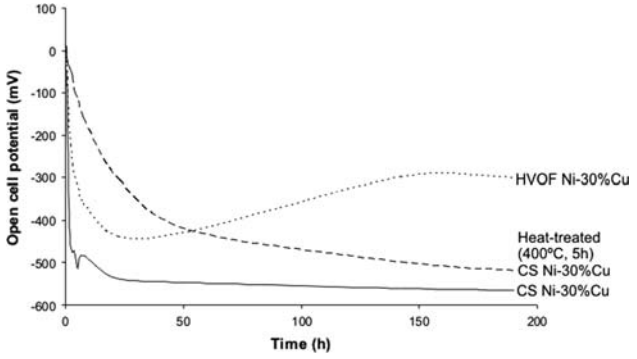

Fig. 15 Open cell potential of cold sprayed Ni-30%Cu coatings as-sprayed and heat-treated (400 °C and 5 h) and HVOF sprayed Ni-30%Cu coating as a function of exposure time

Table 4 Summary of coatings performance in salt spray fog testing

Coating	Time to first change	Final state (96 h)	Comment (96 h)
CS Cu	6 h, several corrosion spots	Pit-type corrosion	Strong rust areas
HVOF Cu	24 h, several corrosion spots	Pit-type corrosion	Strong rust areas
CS Ni	48 h, some local corrosion spots	Pit-type corrosion	Partly clean and rust areas
HVOF Ni	No changes	No corrosion products	...
CS Ni-30%Cu	6 h, several corrosion spots	Pit-type corrosion	Partly clean and rust areas
HVOF Ni-30%Cu	96 h, some local corrosion spots	Few rust areas	Local rusty areas

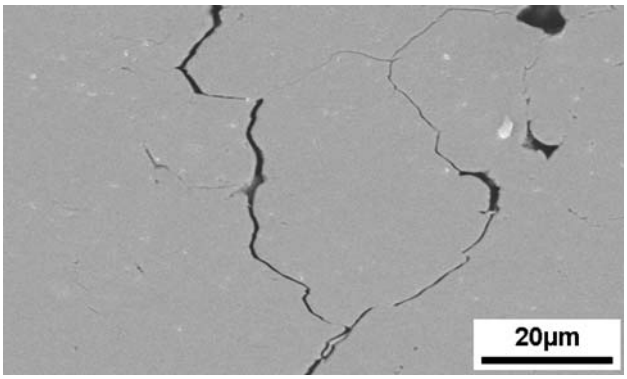

Fig. 16 Cold sprayed Ni-30%Cu coating after salt spray testing. Particle boundaries seemed to be open in some parts of the coating

HVOF coatings were found to have slightly better corrosion resistance than the cold sprayed coatings. Figure 16 presents the microstructure of the cold sprayed Ni-30%Cu coating after the salt spray test. Inter-particle boundaries seem to be also more open in the some areas of the coating than in the as-sprayed coating.

The salt spray corrosion tests showed clearly that all cold sprayed coatings were not fully protective and the coatings seemed to contain a varying amount of local defects. These areas acted as routes along which the salt solution was able to penetrate to the coating-substrate interface. It was also found that the surfaces of the cold sprayed coatings could typically have both areas with corrosion products but also areas free of these. It is apparent that the clean areas with no corrosion products reflect dense coatings with nearly perfect microstructures. Despite of the dense microstructures, as observed by SEM, the cold sprayed Ni and Ni-30%Cu coatings seemed not to be fully protective and perfect corrosion barriers due to some through-porosity present in the coatings. It is evident that more coating improvement and optimization is needed in order to produce fully protecting corrosions barriers. The HVOF sprayed coatings were found to be dense or to contain through-porosity, depending on the coating, see Table 4.

4. Discussions

4.1 Microstructure of Cold Sprayed Coatings

The cold sprayed coatings seemed to be dense according to microstructural studies of unetched coating specimens by SEM, see Figs. 6a, 9a and 10a. Pores, other voids or inter-particle boundaries were not detectable unless the coatings specimens were chemically etched. Therefore, more detailed information about the real microstructure could be obtained only from etched specimens, see Figs. 6c, 8a, 9b and 10c. Only chemical etching could reveal the inter-particle boundaries, microstructure inside the spray particles, more detailed characteristics such as slip bands or grain boundaries, and degree of deformation of the sprayed powder particles. In the cross-sectional specimen, the sprayed particles were strongly flattened due to high impact velocities of the sprayed powder particles. Deformation during cold spraying presents in the form of slip bands in the coating particles are seen to some extent in the etched microstructures. However, the actual grain size within the particles is not clearly seen. Calla et al. (Ref 5) have reported that notably degrees of grain refinement in cold spraying as compared to the original Cu powder can occur. Etching of the coating microstructure has also been reported to show highly localized particle deformation (Ref 9). Our studies showed that the interface between the coating and the substrate seemed to be almost faultless, which is known to be typical to cold sprayed coatings, see e.g., Fig. 10a. This clearly proves that the sprayed powder particles adhere well to the surface of the substrate. Moreover, the cold sprayed Ni-30%Cu coating appeared to be dense, because all particle boundaries are not clearly seen in the etched specimen.

Chemical etching of the cross-sectional coating specimen was found to be very challenging because of the different coating and substrate materials. Different nobleness of the coatings and the substrates affects the etching behavior in the cross-sectional specimen. Galvanic couples tend to form between the coating and the substrate in the presence of the chemical etching electrolyte. The steel substrate behaved sacrificially as compared to the cold sprayed Cu coating influencing that the coating did not become etched uniformly equally all around the cross-section, see Fig. 6b. Furthermore, the cold sprayed Cu coating tends to become etched more on the top of the coating as compared to the interface between the coating and the substrate. This influence in different etching behavior was eliminated in the polished specimen with top view of the coating, but obviously the microstructures are very different due to different viewing directions. The shapes of the flattened and deformed particles are only seen from the cross-sectional view and not directly from the top-view. However, the top-view examination of the cold sprayed coating particles gives a better possibility to

evaluate the microstructure inside the particles as well as gives some useful information about adhesion and voids present between the sprayed particles or splats. Such voids can be detrimental to the protectiveness of the coating in corrosive environments.

Heat treatment affects microstructures and properties of the cold sprayed coatings. Heat treatment affected coating properties through the well-known by recovery, recrystallization and grain growth mechanisms. After a heat treatment at 200 °C for cold sprayed Cu coating, some recrystallization has possibly taken place showing signs of noticeably lower amount of slip bands, see Fig. 7a. Moreover, even less slip bands are observed in a cold sprayed Cu coating heat-treated at 400 °C, Fig. 7b. In the case of cold sprayed Ni-30%Cu coatings the effect of heat treatment on the microstructure appeared as different chemical etching behavior under similar etching conditions. Degrees of etching of cold sprayed Ni-30%Cu coating decreased significantly with increased heat treatment temperature, which indicates denser coating with a lower amount of inter-particle voids. Recovering is known to restore work hardening and the mechanism prevailing is the reduction of internal energy by dislocation rearrangement. After recovery the grains are still in a relatively high strain energy state. Recrystallization further decreases internal energy. Metals become softer and more ductile during recrystallization; the properties then depend on both the time and the temperature of the heat treatment. The degree of recrystallization is known to increase with time (Ref 10). At the heat treatment temperatures 200-300 °C for cold sprayed Cu coating, hardness was found to decrease and correlating with the recrystallization and thus softening of the coating material (Ref 11). Moreover, recrystallization is also seen in the microstructures of heat-treated cold sprayed coatings by different etching degrees. The heat treatment temperature 200 °C for cold sprayed Cu coating has been indicated to cause recrystallization according to Stoltenhoff et al. (Ref 9). Also they have reported that recrystallization is mainly focused at the temperature of 200 °C on strongly deformed areas. Recrystallization tends to occur more rapidly in pure metals than in metal alloys, i.e., alloying tends to raise the recrystallization temperatures (Ref 10).

4.2 Denseness and Corrosion Characteristics of Cold Sprayed Coatings

The aim of the corrosion tests was to investigate the denseness and especially the presence of through-porosity of the cold sprayed coatings. Through-porosity is critical to Cu, Ni, and Ni alloy coatings because these coatings are known to protect anodically the steel substrates against the potential corrosion attack. Production of fully dense coatings plays an important role in creating corrosion resistant and protective coatings. In this work, possibly existing through-porosity and local weak areas in the cold sprayed coatings was revealed by corrosion testing. Measurement of the open cell potentials with time of immersion could show the existing through-porosity by comparison of the potentials of coatings on substrates and reference materials, i.e., the corresponding bulk/wrought material and the carbon steel substrate. Another methods used was conventional salt spray fog testing. In this test the surfaces were studied by visual inspection of the corrosion products originating from the substrate at the interface of the coating and the substrate.

According to the open cell potential measurements cold sprayed Cu coatings prepared from slightly coarser powders, i.e., BSA $-38+11$ μm and Osprey $-30+10$ μm, were fully dense and no defects or voids were observed. Open cell potentials of these cold sprayed Cu coatings were found to be similar with the values of bulk Cu, as is presented in Fig. 13. Obviously, the powder characteristics can affect the impermeability of cold sprayed Cu coatings. The cold sprayed Cu coatings prepared from the coarser powders were dense also according to the open cell potential measurements. The cold sprayed Cu coating prepared from the finer powder (BSA $-22+5$ μm) behaved somewhat weaker than the other cold sprayed Cu coatings. Some through-porosity was found to be in this cold sprayed Cu coating. However, it should be noticed that this cold sprayed Cu ($-22+5$ μm) coating performed still better than HVOF sprayed Cu coating, although as well as the other cold sprayed Cu coatings. The cold sprayed Cu coating ($-22+5$ μm) seemed to contain some local defects according to both corrosion tests. Apparently the salt spray solution could easily found a way to penetrate to the substrate surface and corrosions products were noticed to be present on the surface of the coating. To summarize the results, fully dense Cu coating can be cold sprayed with optimum size spray powder, in this work with the coarser powder, and also with the warmer cold spraying parameters, i.e., a higher gas preheating temperature. It is possible that lower preheating temperature with finer Osprey Cu powder had an influence to the results of the corrosion tests. Process temperature can affect to the particle velocity meaning lower velocity with lower temperature. The temperature can have an influence to the denseness of the coating in the cold spraying process. Microstructure can be denser spraying with warmer parameters affecting better results during corrosion tests.

Also cold sprayed Ni and Ni-30%Cu coatings seemed to be dense according to the SEM analysis. Although the coatings appeared to be microstructurally dense, the cold sprayed Ni and Ni-30%Cu coatings showed through-porosity in the some parts of the coatings according to the corrosion tests. Some weak-points were between weakly bonded particle interfaces (pores); all particles were not well enough deformed and adhered to result in the most perfect coatings, see Figs. 12 and 16. The cold sprayed coatings contained through-porosity in the some parts of the coatings and inter-particle boundaries seemed to be more open in the some areas of the coating (Fig. 16). The bonding between the particles is stronger in the more closed areas of the particle boundaries than in the open boundaries. Pit-type corrosion areas were found to be typical to cold sprayed coatings on the coating by the surface examination during and after the corrosion tests. Reference HVOF sprayed coatings were noticed to be dense like HOVF Ni coating or to contain through-porosity like HVOF Cu and

Ni-30%Cu coatings. Some cold sprayed coating areas did not leak (clean and corrosion product-free surfaces) giving a potential to develop also even fully dense Ni and Ni-30%Cu coatings by cold spraying. This is assumed to be able to be reached by powder development and by substrate-coating pairs character balance. Effect of heat treatment to denseness was also tested with cold sprayed Ni and cold sprayed Ni-30%Cu coatings. In open cell potential measurement, cold sprayed Ni coating became denser after heat treatment because of recrystallization and softening possible due to that rearrangement of grains close the pores. Open cell potential of cold sprayed Ni coating was near to value of electrolytically deposited Ni coating indicating denser microstructure. In the case of heat-treated (400 °C) cold sprayed Ni-30%Cu coating, open cell potential (Fig. 15) did not change needing more research and development.

5. Conclusions

This study concentrated in microstructural studies of cold sprayed copper, nickel, and nickel-30%copper coatings. SEM analysis and corrosion tests were done to get more information about denseness of the coatings and characteristics of the spray particle boundaries. The cold sprayed coating seemed to be dense by microstructural examination. The interface between the coating and the substrate seemed to be fairly faultless. To reveal the real microstructure, coatings had to be etched to see the particle boundaries, deformation and microstructure inside the sprayed particles. Cold sprayed Cu coatings (coarser particle size) were dense according to SEM analysis and open cell potential measurements, indicating fully dense Cu coatings producible by cold spraying. Cold sprayed Ni and Ni-30%Cu coatings seemed also to be dense according to the SEM studies. However, corrosion tests showed some through-porosity in the cold sprayed Ni and Ni-30%Cu coatings. It was noticed that the weak-points were on the particle boundaries where the bonding is not strong and uniform enough between the particles. Areas with corrosion products and clean uncorroded surface areas after corrosion tests were found to be typical for the cold sprayed coatings. Moreover, those clean areas showed that the possibility to produce fully dense Ni and Ni-30%Cu coatings by cold spraying. Furthermore, cold sprayed Ni coating became denser after heat treatment (400 °C, 5 h) because of pores closuring by rearrangement of grains and softening. Further research should be focussed to development and optimization of the spray powders as well as in optimization of the cold spray parameters and process to produce microstructurally fully dense coatings. Such examinations should also include SEM analysis and corrosion tests to be able to detect the real protectiveness of the coatings.

Acknowledgments

The authors would like to thank Mr. Werner Krömmer from Linde AG Gas for spraying coatings and for valuable discussions. The work in which this study was done was funded by The National Technology Agency of Finland (Tekes) and some Finnish industrial companies.

References

1. T. Stoltenhoff, H. Kreye, and H.J. Richter, An Analysis of the Cold Spray Process and its Coatings, *J. Therm. Spray Technol.*, 2001, **11**(4), p 542-550
2. T.H. Van Steenkiste, J.R. Smith, and R.E. Teets, Aluminum Coatings via Kinetic Spray with Relatively Large Powder Particles, *Surf. Coat. Technol.*, 2002, **154**, p 237-252
3. R.C. Dykhuizen and M.F. Smith, Gas Dynamic Principles of Cold Spray, *J. Therm. Spray Technol.*, 1998, **7**(2), p 205-212
4. C. Borchers, F. Gärtner, T. Stoltenhoff, H. Assadi, and H. Kreye, Microstructural and Macroscopic Properties of Cold Sprayed Copper Coatings, *J. Appl. Phys.*, 2003, **93**(12), p 10064-10070
5. E. Calla, D. G. McGartney, and P.H. Shipway, Effect of Heat Treatment on the Structure and Properties of Cold Sprayed Copper, *Thermal Spray 2005: Explore its Surfacing Potential!*, ASM International, May 2-4, 2005 (Basel, Switzerland), ASM International, 2005
6. K. Balani, T. Laha, A. Agarwal, J. Karthikeyan, and N. Munroe, Effect of Carrier Gases on Microstructural and Electrochemical Behavior of Cold-sprayed 1100 Aluminum Coating, *Surf. Coat. Technol.*, 2005, **195**, p 272-279
7. R. E. Blose, D. Vasquez, and W. Kratochvil, Metal Passivation to Resist Corrosion using the Cold Spray Process, *Thermal Spray 2005: Explore Its Surfacing Potential!*, ASM International, May 2-4, 2005 (Basel, Switzerland), ASM International, 2005
8. "Standard Test Method of Salt Spray (Fog) Testing," B117-90, Annual Book of ASTM Standards, ASTM, p 19-25
9. T. Stoltenhoff, C. Borchers, F. Gärtner, and H. Kreye, Microstructures and Key Properties of Cold-sprayed and Thermally Sprayed Copper Coatings, *Surf. Coat. Technol.*, 2006, **200**, p 4947-4960
10. W. D. Callister, *Materials Science and Engineering*, 5th ed, John Wiley & Sons, Inc. 2000, 871 p
11. J. Lagerbom, H. Mäkinen, and P. Vuoristo, Effect of Heat Treatment on Properties of Cold Sprayed Coatings, *Thermal Spray 2005: Explore Its Surfacing Potential!*, ASM International, May 2-4, 2005 (Basel, Switzerland), ASM International, 2005